13th Australasian Fluid Mechanics Conference
Monash University, Melbourne, Australia
13-18 December 1998

BUBBLE TRAJECTORY BIFURCATIONS IN CROSS FLOW

Richard MANASSEH, Shizuo YOSHIDA* & Naohiko KAJIO*

Advanced Fluid Dynamics Laboratory
CSIRO BCE, PO Box 56, Highett, VIC 3190, Melbourne, AUSTRALIA

* Laboratory of Physical Fluid Mechanics
Graduate School of Engineering, Hokkaido University, Sapporo 060, JAPAN

ABSTRACT

Experimental results on the trajectories of bubbles in cross flow are presented. The bubbles were produced by a continuous stream of air fed into a water tunnel from an underwater nozzle. Comparative studies were first made in quiescent liquid. The trajectories exhibit an interesting bifurcation, where bubbles alternately enter either one sinusoidal path or the other.

INTRODUCTION

Continuous gas sparging and cross-flows are typical of many practical cases, in which the bubble trajectory has an important effect on the rate of mass transfer between gas and liquid. Industrial applications are aeration systems in minerals processing, polymer manufacture and metallurgy, and also beverage industries, wastewater treatment, and aquaculture. In the ocean, bubble trajectories under breaking waves influence absorption of atmospheric carbon dioxide.

Descriptions of the rise of individual medium-sized bubbles (between 1 and 10 mm diameter) can be found in many references (for example, Clift *et al* 1978). When bubbles are formed from an underwater nozzle, they initially rise in a straight line. During this phase, the bubble shape undergoes both initial volumetric oscillations and subsequent axisymmetric shape oscillations. It is well known that bubbles emit an acoustic signal during the volumetric oscillations and that the frequency of the signal can be used to calculate the bubble radius r_0 (Minnaert 1933; see Manasseh *et al* 1998 for recent references). Such calculations are often the most accurate way of determining bubble size and gas flow rate (Manasseh 1997).

When the bubbles reach a particular height they form an ellipsoidal shape in which all axes are tilted away from the vertical. They then rise on a trajectory that has been described as spiral or zig-zag (Lunde & Perkins 1997). Details of these bubble trajectories are the subject of active research, with many uncertainties as to their dynamics. For example, Lunde (as reported in Leighton, 1994, pp 123–124) showed that a single bubble can follow a zig-zag trajectory, coordinated with vortex shedding behind the bubble. However, he showed that under the same experimental conditions, the bubble might also spiral, without vortex shedding. It was noted by Lunde & Perkins (1997) that single bubbles do not necessarily follow a simple spiral or zig-zag trajectory. They also observed a single bubble changing from a zig-zag to a spiral as it rose.

In most industrial contexts, bubbles are not produced singly but under continuous sparging. Such streams of bubbles may behave in a more complex fashion, or even more deterministically, owing to the mutual influence of bubble wakes and shape oscillations, and the proximity of other bubbles. The lateral motion of bubbles may contribute significantly to the turbulence generated by bubbles in mixing situations. Furthermore, the overall length of the trajectory influences the residence time of the bubble in the liquid. This is very important for gas absorption. The present paper investigates the nature of the trajectories when a stream of bubbles is produced in both quiescent liquid and under cross-flow conditions.

TRAJECTORIES IN QUIESCENT LIQUID

Experimental Method

The bubbles were produced by a nozzle with a constant-pressure air supply through a precision airflow meter. The bubbles were thus produced in pressure-controlled mode (Chhabra 1993). The nozzles had internal diameters ranging from 0.25 mm to 0.50 mm; with orifices of this size, the actual orifice diameter has little influence on the bubble size, which is controlled by the supply pressure. An acoustic technique (Manasseh 1997) was used to measure the bubble size; this is more accurate than calculating the bubble size using the metered air-flow rate. The vertical rise speed of bubbles around 2–8 mm in

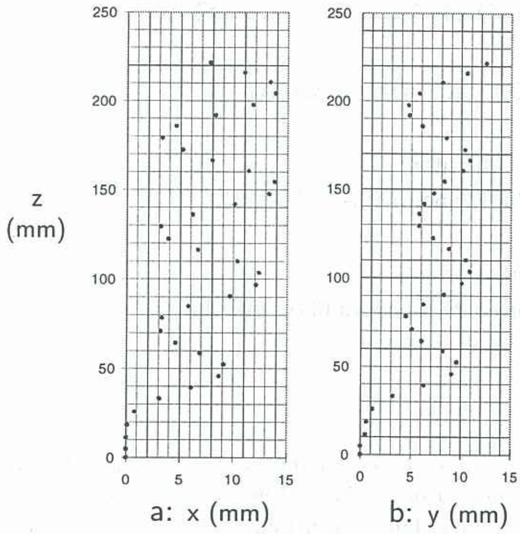

Figure 1: Trajectory of a single bubble released from a 0.4 mm ID underwater nozzle. a: motion projected in x–z plane; b: motion projected in y–z plane. For definitions of x and y, see figure 2.

diameter is quite insensitive to their size and is about 0.3 m s^{-1} (Maxworthy *et al 1996*).

The trajectory of a single bubble

In order to first observe the trajectory of a single air bubble, bubbles were released at quite long intervals and each bubble was then photographed with a strobed light source and a camera. The flashes were set to an interval of 20 milliseconds (50 Hz). Data on the measured trajectory of a typical bubble is shown in figure 1.

Figure 1*(a)* shows the trajectory of the bubble in the x–z plane at 20 ms intervals; figure 1*(b)* shows the trajectory in the y–z plane at 20 ms intervals. Figure 2*(a)* shows the trace of the trajectory projected onto the x–y plane, and figure 2*(b)* shows the trajectory in three dimensions, The chief characteristics of the behaviour are:

1. The bubble follows a sinusoidal path, the axis of which is initially near the nozzle, at a position of about $x = 5$ mm, $y = 5$ mm. However, the axis shifts away from the nozzle as the bubble rises in the z-direction, reaching about $x = 9$ mm, $y = 9$ mm when the bubble is at the water surface. The trajectory is a spiral.

2. The length of a single helix of the trajectory, projected on the x-axis, is about 25 mm. Since the acoustically-determined diameter of the bubble is 2.19 mm, this corresponds to 10.5 times the bubble diameter. The single-helix length projected on the y-axis is initially about 25 mm, but this increases as the bubble rises. Thus, as shown in figure 2*(a)*, the spiral path has an elliptical cross-section. The vertical 'wavelength' of the spiral is about 50 mm (25 diameters).

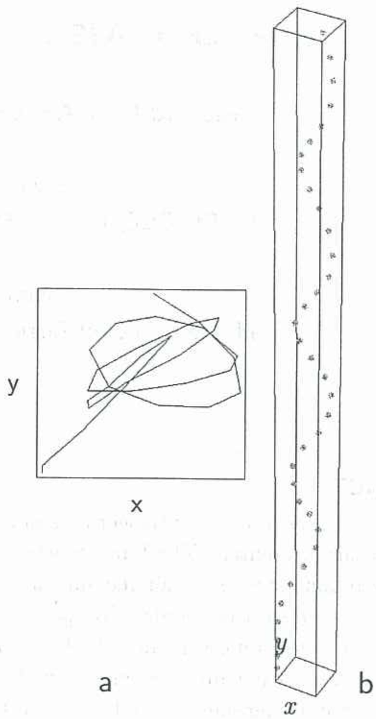

Figure 2: Trajectory of a single bubble released from a 0.4 mm ID underwater nozzle. (a): motion projected in x–y plane; (b) 3-D view.

3. The data in figure 2*(a)* show that the length of the major axis of the spiral does not change much. The minor axis increases with upward (z-direction) movement of the bubble, from a near-zero value in the vicinity of the nozzle, and the bubble approaches a circular path. It also appears that the elliptical path is itself precessing clockwise in the x–y plane.

Trajectories of continuously-sparged bubbles

When bubbles under continuous sparging begin to follow a spiral path, its trajectory in fact bifurcates into two spirals at a critical height. Alternate bubbles enter first one, then the other spiral. The two spirals are intertwined helices, similar to the double helix of DNA. This was noticed by Yoshida & Manasseh (1997) for larger bubbles; they also detailed a primary and secondary structure to the trajectory. Furthermore, at higher sparging rates, the trajectory may divide into many trajectories, not just two. Full

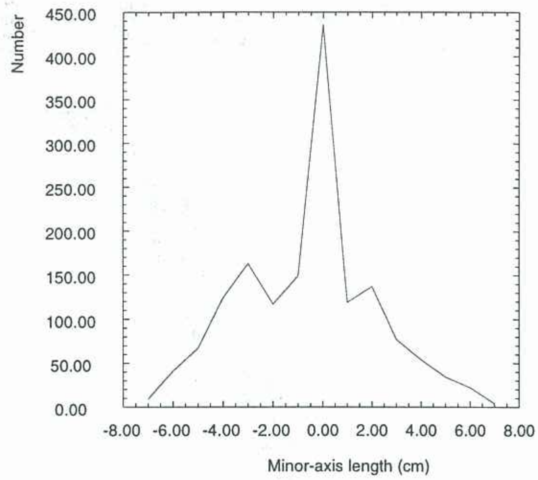

Figure 3: Histogram of the minor-axis length of trajectories of bubbles continuously sparged from a 0.25 mm ID underwater nozzle.

details of this behaviour are given in Yoshida *et al* (1998).

A total of 1557 bubbles were continuously observed under continuous-sparging conditions. The lengths of the minor axes of the helices traced by each bubble, projected onto the water surface, were plotted to create the histogram shown in figure 3.

Positive values of the minor axis indicate that the bubble rose in a counterclockwise motion; negative values that the bubble rose in a clockwise motion. These results show that the minor axis most often had a length of zero. In other words, these zero-minor-axis bubbles rose in a plane. This will be described as a 'planar sinusoidal', rather than a 'zig-zag' trajectory, because the bubbles followed a smooth, sinusoidal path and did not turn sharply onto each new tack, as the term zig-zag suggests. There were also smaller peaks on either side of the zero-value peak. The selection of a clockwise or counterclockwise helix was not random; if one bubble rose in a clockwise helix several of the following bubbles would follow the leader. Furthermore, the transition from clockwise to counterclockwise (or vice versa) was not abrupt; it would proceed through a sequence of helices with gradually shrinking minor axes, and then a period of planar trajectories, before changing to the other sense of rotation.

Thus, as the minor axis length passed through zero, a transition occurred from a helix 'wound' in one sense to one of the opposite sense. Similar behaviour has been noted for bubbles ranging in size from about 2.0 to 4.5 mm (Yoshida & Manasseh 1997).

TRAJECTORIES IN CROSS FLOW

Experimental Method

Bubbles were released in pressure-controlled mode as described above, but this time into a water tunnel. The working section was 0.305 m wide and filled to a depth of 0.257 m. The bubbles were released from a point 0.2 m from the start of the working section and from a machined orifice of 0.5 mm ID at the tip of a rod 6.35 mm in diameter. The orifice was 33 mm above the floor of the tunnel. Water flow speeds varied from zero to 0.28 m s^{-1}. At the maximum speed, the boundary-layer Reynolds number was about 56000 at the orifice location. This means the boundary layer here was always in the laminar regime, and the maximum boundary-layer displacement thickness, calculated from well-known results (Blevins 1992), is about 1.5 mm. Hence, the bubbles were released well into the free stream and their dynamics can be assumed free of wall effects.

The bubbling rate (rate of bubble production) was measured at each cross-flow speed with a strobe. The bubble acoustic frequency with zero cross flow was used to calculate the bubble volume. This acoustically-measured volume, multiplied by the bubbling rate, gives the air flow rate more precisely than most flow meters (Manasseh 1997). The hydrophone was not introduced into the system with the cross flow running, to avoid disturbing the flow and also because electrical noise from the pump controller made measurements difficult. However, the air supply system maintained the same air-flow rate irrespective of cross-flow speed, so the measured bubbling rate at each cross flow could be used to calculate the bubble volume at each cross-flow rate.

Cross-flow results

For these experiments, the bubbling rate with no cross-flow was 32.6 ± 1.0 Hz. The corresponding bubble mean diameter was acoustically determined to be 4.25 ± 0.04 mm. Bubbles of this size, continuously sparged, spiral with a vertical wavelength of about 11 bubble diameters (Yoshida and Manasseh 1997). Following the bubble as it rises vertically at 0.3 m s^{-1}, the frequency of trajectory oscillation is about 6–7 Hz.

Figure 4 shows the view from the top and side, with a cross flow of 0.18 ± 0.01 m s^{-1}. With this cross-flow speed and the same total air flow rate, the bubbling rate increases to 44.4 ± 1.0 Hz. Hence, the bubble volume is about 25% less; and the bubble diameter is reduced to 3.8 ± 0.1 mm. This reduction in bubble volume due to cross flow compares well with the results of Marshall *et al* (1993).

The exposure of the top view in figure 4 is over 1/4 s while the side view is over 1/8 s. Both im-

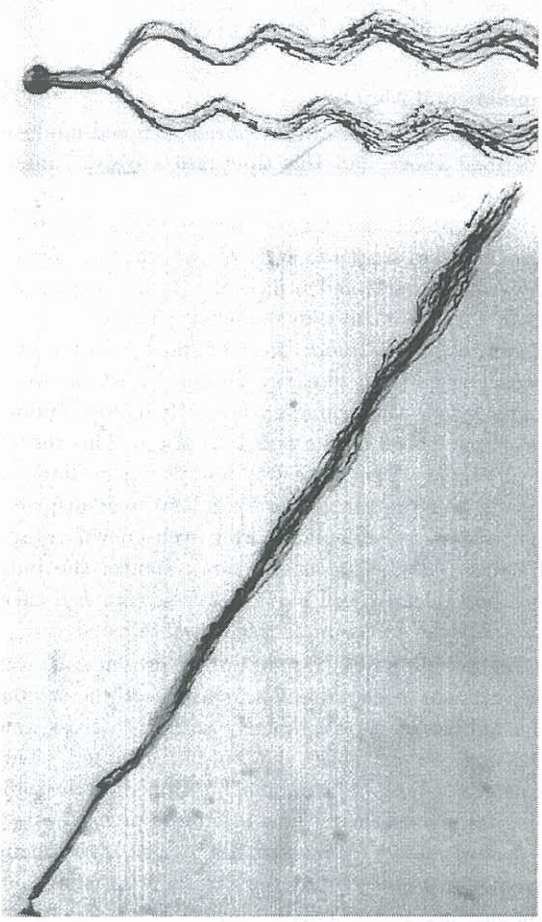

Figure 4: Bubble trajectories at an 'ideal' cross-flow speed, viewed from above and side. Cross-flow speed 0.18 ± 0.01 m s^{-1}.

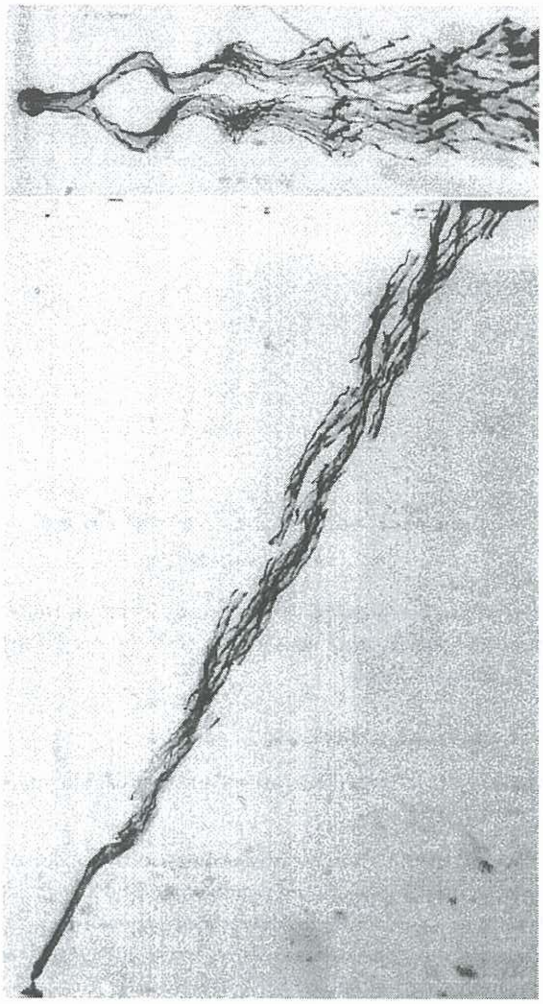

Figure 5: Bubble trajectories in low cross flow; cross-flow speed 0.14 ± 0.01 m s^{-1}.

ages cover 0.15 m in the streamwise direction. The two paths have clearly separated after the bifurcation point and form a pair of sinusoidal paths. Successive bubble trajectories closely re-trace each other. This cross-flow speed gives an 'ideal' pattern: the clearest separation of the pair of trajectories.

There is a slight phase difference between the two trajectories. The side view shows that the trajectories are effectively co-planar. The wavelength is approximately 0.030 m (8 diameters) projected onto a horizontal plane, or 0.055 m (15 diameters) in the plane of the trajectories. The frequency of trajectory oscillation, following the bubble, is about 5–6 Hz; it has not significantly changed from the quiescent case.

The behaviour at lower cross-flow speeds (0.14 m s^{-1}) is shown in figure 5. In this case the bubble diameter is 4.0 ± 0.1 mm, only marginally less than in quiescent conditions. The bifurcation still occurs, but after the first sinusoidal period the trajectories virtually overlap. The trajectories after the first sinusoidal period show more variability; they do not closely re-trace the same path. The frequency of trajectory oscillation, following the bubble, is still about 5–6 Hz.

At higher speeds (0.22 m s^{-1}; figure 6), the trajectories also show more variability. The bubble diameter has been reduced to 3.6 ± 0.1 mm. The frequency of trajectory oscillation is about 5-6 Hz. The 'bifurcation' point still exists, but represents a transition to multiple trajectories. Nevertheless, at both high and low speeds the basic sinusoidal periodicity dominates the trajectories. At even higher speeds a regime exists in which the trajectory pattern intermittently changes from asymmetric, sinusoidal paths to symmetric paths.

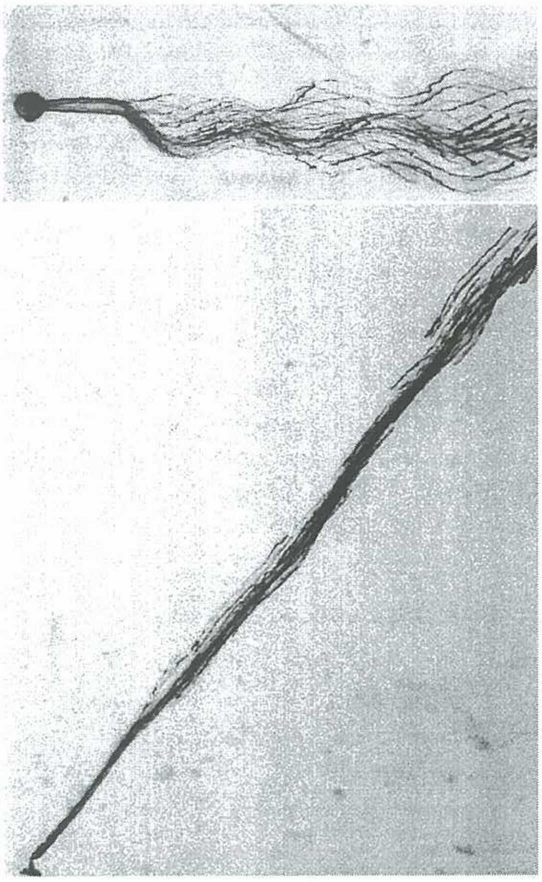

Figure 6: Bubble trajectories in high cross-flow; cross-flow speed 0.22 ± 0.01 m s^{-1}.

DISCUSSION & CONCLUSION

The spiralling behaviour of bubbles and the existence of a trajectory bifurcation point may be explained by the following qualitative mechanism, which remains untested.

Initially, the bubble rises a few diameters vertically, while undergoing axisymmetric shape oscillations. (Also during this time, it is emitting an acoustic signal.) The shape oscillations can be described as capillary-wave oscillations of the bubble. At a critical height, the bubble establishes an ellipsoidal shape with at least one of its axes non-vertical. Once the bubble has this shape, the liquid around it will experience a sideways 'lift' force (as long as the bubble rises with at least one non-vertical axis), owing to the shape of the streamlines around it. Therefore the liquid around it will begin to accelerate sideways.

The existence of a bifurcation under continuous sparging may be due to the wake of the bubble. Once a bubble begins to move sideways, the liquid in its wake will have a sideways component. Hence, the following bubble is rising into a wake with a sideways component. According to Chen *et al* (1998), the leading bubble's wake elongates the following bubble, so that its major axis becomes normal to the major axis of the leading bubble. The following bubble is therefore likely to be distorted into an ellipsoid oriented such that it moves sideways in the opposite sense to the leading bubble. Thus, successive bubbles enter alternate trajectories.

As the sideways velocity increases, hydrodynamic forces begin to distort the bubble shape, eventually limiting the bubble's sideways motion. Capillary oscillations of the bubble shape, locked to the timescale over which the bubble accelerates sideways, will tend to reverse the orientation of the major axis, reversing - or re-directing - the sideways motion. It is clear that this mechanism permits periodic, three-dimensional solutions, such as a spiral, This mechanism also implies the existence of a natural spiralling frequency, dependent on bubble size. However, much further research is required to test the validity of this mechanism.

In a cross flow, there are additional periodic factors which may influence the trajectories. The stream of continuously-sparged bubbles is effectively a buoyant jet in a cross flow, albeit one composed of discrete and immiscible 'quanta' of buoyancy. Studies such as that of Kelso *et al* (1996) show that periodic 'horseshoe' vortices may form in the wake of a round jet in a cross flow. For the conditions of figure 4 the bubble centres are about two diameters apart, so neither an inclined-round-jet nor an isolated-bluff-body approximation will be wholly valid. Moreover, the generation of wake vorticity from a column of bubbles, which lacks a solid boundary, will not be as straightforward as from solid cylinder.

The Reynolds number based on the bubble diameter is about 800. Persevering with the assumption of wake vortices from the bubble 'column', the Strouhal number (St) is about 0.2 for vortex shedding from an inclined cylinder (Blevins 1992). An estimate of the frequency f of the wake disturbance could be made using $f = \mathrm{St}U/d_s$ where U is the cross-flow speed and d_s is an appropriate length scale. This gives about 7.6 Hz for the inclined cylinder approximation (taking d_s as the sliced-cylinder's diameter projected on the horizontal). This compares with 6–7 Hz for the cross-flow observation. (Recall that the bubbles were produced by a short rod about 1/10 the water depth; this should shed vortices at a similar frequency of 5.8 Hz, though these vortices may not propagate over the entire depth of the bubble 'column'.)

Thus, at the 'ideal' cross-flow speed of figure 4, wake oscillations would have the right frequency to interact with the bubble's natural spiralling frequency in quiescent liquid (6–7 Hz). In comparison, the slow cross-flow case of figure 5 represents a similar 'Strouhal frequency' of 6.1 Hz while the high cross-flow of figure 6 gives 9.9 Hz.

In summary, the bifurcation of bubble trajectories is a robust phenomenon under both quiescent and cross-flow conditions. The sinusoidal nature of the trajectories observed in quiescent liquid is preserved under cross flow. The cross flow seems to stabilize the trajectories' helical minor axis at or near zero; in other words, the trajectories are co-planar. However, a clear separation of the pair of trajectories only occurs for a narrow regime of cross-flow speeds. This may correspond to a resonance between a natural bubble spiralling frequency and oscillations of the wake.

REFERENCES

BLEVINS, R. D. *Applied Fluid Dynamics Handbook* Krieger, Florida, USA, 1992.

CHEN, L., LI, Y. and R. MANASSEH, "The coalescence of bubbles - a numerical study", *3rd International Conference on Multiphase Flow, Lyon, France, paper 626.*, June 1998.

CHHABRA, R. P., *Bubbles, Drops, and Particles in non-Newtonian Flows,* CRC Press, Boca Raton, Florida, USA, 1993.

CLIFT, R., GRACE, J. R. and M. E. WEBER, *Bubbles, drops and particles.* Academic Press, London, 1978.

KELSO, R. M., LIM, T. T., A. E. PERRY, "An experimental study of round jets in cross flow", *J. Fluid Mech.* **306**, 111–144.

LEIGHTON, T. G., *The Acoustic Bubble,* Academic Press, London, 1994.

LUNDE, K. and R. J. PERKINS, "Observations on wakes behind spheroidal bubbles and particles", *Proceedings, ASME Fluid Engineering Division Summer Meeting,* 22–26 June 1997.

MANASSEH, R., "Bubble-pairing phenomena in sparging from vertical-axis nozzles", *Proceedings, 24th Australian & NZ Chemical Engineering Conference, Sydney, 30 Sep - 2 Oct,* **5**, 27–32, 1996.

MANASSEH, R., "Acoustic sizing of bubbles at moderate to high bubbling rates", *Proc. 4th World Conference on Experimental Heat Transfer, Fluid Mechanics and Thermodynamics,* Brussels, 2–6 June 1997.

MANASSEH, R.,YOSHIDA, S. and M. RUDMAN, "Bubble formation processes and bubble acoustic signals", *Proceedings, Third International Conference on Multiphase Flow, Lyon, France, 8–12 June 1998.*

MARSHALL, S. H., CHUDACEK, M. W. & BAGSTER, D. F. "A model for bubble formation from an orifice with liquid cross-flow", *Chem. Eng. Sci.* **48**(11), 2049–2059, 1993.

MINNAERT, M. "On musical air bubbles and the sound of running water", *Phil. Mag.*, **16**, 235–248, 1933.

YOSHIDA, S. & MANASSEH, R., "Trajectories of rising bubbles", *Proceedings, the 16th Japanese Multiphase Flow Symposium,* Touya, Hokkaido, July 1997.

YOSHIDA, S., MANASSEH, R., and N. KAJIO, "The structure of bubble trajectories under continuous sparging conditions", *Proceedings, Third International Conference on Multiphase Flow, Lyon, France, 8–12 June 1998.*

MAXWORTHY, T., GNANN, C., KÜRTEN, M. and F. DURST, "Experiments on the rise of air bubbles in clean viscous liquids", *J. Fluid Mech.* **321**, 421–441, 1996.